One-pot synthesis of pH-responsive Eudragit-mesoporous silica nanocomposites enable colonic delivery of glucocorticoids for the treatment of inflammatory bowel disease

Qu, Zhi

2021-02

Qu , Z , Wong , K Y , Moniruzzaman , M , Begun , J , Santos , H A , Hasnain , S Z , Kumeria , T , McGuckin , M A & Popat , A 2021 , ' One-pot synthesis of pH-responsive Eudragit-mesoporous silica nanocomposites enable colonic delivery of glucocorticoids for the treatment of inflammatory bowel disease ' , Advanced Therapeutics , vol. 4 , no. 2 , 2000165 . https://doi.org/10.1002/adtp.202000165

http://hdl.handle.net/10138/335107
https://doi.org/10.1002/adtp.202000165

acceptedVersion

ADVANCED THERAPEUTICS
www.advtherap.com

One-Pot Synthesis of pH-Responsive Eudragit-Mesoporous Silica Nanocomposites Enable Colonic Delivery of Glucocorticoids for the Treatment of Inflammatory Bowel Disease

*Zhi Qu, Kuan Yau Wong, Md. Moniruzzaman, Jakob Begun, Hélder A Santos, Sumaira Z. Hasnain, Tushar Kumeria, Michael A. McGuckin, and Amirali Popat**

Oral glucocorticoids are backbones for the acute management of inflammatory bowel disease (IBD). However, the clinical effectiveness of conventional oral dosage forms of glucocorticoids is hindered by their low delivery efficiency and systemic side effects. To overcome this problem, a smart drug delivery system with high loading capacity and colonic release by coating functionalized mesoporous silica nanoparticles (MSNs) with a pH-responsive polymer Eudragit S100 is proposed. In vitro dissolution tests show that Eudragit-coated MSNs can limit the burst release of loaded prednisolone and budesonide in the gastric environment with more than 60% of the drugs released only at colonic pH (i.e., pH $\geq$ 7). In vivo therapeutic efficacy of budesonide-loaded nanoparticles is tested in a murine model of dextran sodium sulfate-induced colitis. An oral budesonide dose of 0.2 mg kg^{-1} nanoparticles with Eudragit coating improves the disease activity index compared to other groups. Interestingly, both coated and uncoated nanoparticles show pathological improvements demonstrated by similar levels of histological colitis score. However, coated nanoparticles significantly decrease mRNA expression of the cytokines (*Il-1β*, *Il-17*, and *Il-10*) particularly in proximal colon, indicating colonic delivery. Overall, this study demonstrates the effectiveness of a simple method to fabricate targeted nanomedicine for the treatment of IBD.

1. Introduction

Inflammatory bowel diseases (IBD) are a group of chronic inflammatory conditions of the intestinal tract.[1] Ulcerative colitis (UC) and Crohn's disease (CD) are the two main forms. IBD affect more than 7 million people across the world, with an annual economic burden of 15 billion USD.[2] Although a range of genetic, immunological, and environmental factors are known to play a role in the development of IBD, the causes of IBD are not yet fully understood.[3] Currently, there is no cure for IBD, and management strategies have focused on inducing and maintaining remission. IBD management typically includes use of amino salicylates, antibiotics, corticosteroids, immunomodulators, and biologics.[4] Corticosteroids are commonly prescribed for acute IBD; however, current corticosteroid medications still result in undesirable systemic side-effects because of the absorption along upper gastrointestinal tract (GIT).[5] Glucocorticoid treatment for IBD is well-known to lead to bone density loss, hyperglycemia, glaucoma, cataracts, skin thinning, impaired growth, adrenal suppression, and steroid dependency.[6]

Dr. Z. Qu, Dr. M. Moniruzzaman, Dr. S. Z. Hasnain, Dr. T. Kumeria, Dr. A. Popat
School of Pharmacy
The University of Queensland
Brisbane QLD 4102, Australia
E-mail: a.popat@uq.edu.au
Dr. Z. Qu, Dr. K. Y. Wong, Dr. S. Z. Hasnain, Dr. T. Kumeria, Dr. A. Popat
Immunopathology Group
Mater Research Institute –The University of Queensland
Translational Research Institute
Brisbane QLD 4102, Australia
Dr. M. Moniruzzaman, Dr. J. Begun
Inflammatory Bowel Disease Group, Mater Research Institute–The University of Queensland
Translational Research Institute
Brisbane QLD 4102, Australia
Dr. J. Begun
Mater Hospital Brisbane
Mater Health Services
South Brisbane QLD 4102, Australia
Prof. H. A Santos
Drug Research Program
Division of Pharmaceutical Chemistry and Technology
Faculty of Pharmacy
University of Helsinki
Helsinki FI-00014, Finland

The ORCID identification number(s) for the author(s) of this article can be found under https://doi.org/10.1002/adtp.202000165

DOI: 10.1002/adtp.202000165

Despite their well-known side-effects, corticosteroids are still used frequently for the treatment of IBD due to their rapid onset of action and effectiveness at inducing remission, compared to other therapeutics, such as immunomodulators and biologics.[7] A potential alternative to oral glucocorticoid delivery is offered by direct rectal therapy, which provides localized treatment for management of IBD in the distal colon.[8] However, rectal administration has poor patient compliance and is not effective for more proximal disease in the colon and small intestine.[9] Considering that most IBD patients require lifelong disease management, oral delivery promises the highest patient compliance and adherence.

The ideal oral drug delivery system for IBD should enable selective and exclusive delivery of drug to the inflamed sites to achieve maximum therapeutic efficacy and limited side-effects. Current strategies include use of prodrugs, such as sulfasalazine, which is activated by bacterial mediated reduction in the distal colon,[10] and coatings of non-starch polysaccharide (COLALPRED, Budenofalk, and Entocort[11]). Obstacles, such as inability to target loaded drug to the diseased tissue, incomplete tablet disintegration, high risk of systemic drug exposure, and high cost associated with injectable biologics are still limiting better management of IBD.[5a,12] Although these strategies provide improved performance, these formulations do not perfectly overcome the above challenges for targeting the inflamed regions in the colon, while avoiding systemic exposure. Hence, new drug delivery technologies for colon targeting are urgently required.

The pH-responsive nanomedicines have been widely used for targeting intracellular compartments in tumors and inflamed tissues.[13] They have distinct advantages for colonic delivery because their properties of drug release at specific pH fit well with the physiological environments of the GIT.[14] Polymers have been extensively investigated for several decades and many pH-responsive polymers have been applied to produce biocompatible nanocarriers.[15] Eudragit S100 polymers are among one of the most studied pH-responsive polymers for oral delivery of small molecules. Eudragit S100 is a commercialized pH-sensitive acrylate for enteric coating for tablets and capsules.[16] It has a dissociation pH above 7, which is suitable for colonic delivery. However, conventional pH-responsive formulations, such as pellets, capsules, and tablets, can be subjected to rapid clearance due to diarrhea, a characteristic of IBD. Diarrhea can lead to decreased GIT residence time and result in incomplete tablet disintegration and rapid excretion, which complicates dosing and impairs therapeutic outcomes.[17]

In this regard, nanoparticles for drug delivery have recently attracted tremendous attention because of their unique ability to passively target the inflamed colon providing local release.[17,18] Moreover, disrupted intestinal barrier at inflamed epithelium provide entrapped particles access from intestinal lumen to the inflamed colonic tissues.[19] Previous studies have found that enhanced therapeutic efficacy can be achieved by utilizing the inflammation-selective adhesion property of nanoparticles in experimental colitis.[20] Based on this, more and more newly designed nanoparticle-based drug delivery systems, such as liposomes, polymers, hydrogels, and inorganic nanoparticles, are developed achieve colon targeted delivery by combining pH-responsive release strategy.[21] However, many of these nanoparticles have poor encapsulation efficiency, suffers from burst release, require costly and complex manufacturing methods.[22]

Mesoporous silica nanoparticles have been studied as drug delivery systems for more than a decade.[23] Advantages include their biocompatibility, high surface area (>1000 m^2 g^{-1}), tunable pore sizes, uniform particle size, large pore volumes, ease of functionalization, and flexibility in loading drugs of different physicochemical properties.[24] The large surface area of mesoporous silica nanoparticles provides rapid adsorption of drug molecules by capillary force.[25] Orally administered silica nanoparticles can be easily excreted or degraded into silicic acid, which is the most bioavailable form of silicon.[26] Another advantage of mesoporous silica nanoparticles is their large loading capacity due to high surface area and large pore volumes. Moreover, numerous of silanol groups on the surface of silica nanoparticles provide perfect binding sites for functional ligands and chemical groups to fulfill specific requirements. Coating of silica nanoparticles can provide drug release based on stimuli, and thus, provide better control of drug release.[22a,27]

Here in, we have developed a one-step rotary-evaporation method for in situ drug loading and pH-responsive coating. Uniform coating and high loading amounts for glucocorticoids, prednisolone, and budesonide were achieved by this method in one-step. In vitro release studies showed that after coating, the loaded drug was mostly released above pH 7 for both glucocorticoids. Budesonide was selected for further in vivo efficacy study of drug-loaded particles on a dextran sodium sulfate (DSS) murine model since in our in-house testing prednisolone did not reverse DSS-induced inflammation in mice.[28] Histological assessment of colonic tissues showed that the nanoparticle-encapsulated budesonide significantly reduced inflammation compared to free budesonide. At biochemical levels, the mRNA expression of cytokine *Tnf-α* and *interleukins (IL)-1β*, *Il-10,* and *Il-17* of pro-inflammatory and anti-inflammatory cytokines indicate significantly greater reduction in the pro-inflammatory cytokine levels in the case of Eudragit S100 coated particles, confirming our hypothesis.

2. Results and Discussion

2.1. Characterization of Mesoporous Silica Nanocomposites

Schematic describing our one-pot pH-responsive mesoporous silica nanoparticles is shown in Scheme S1, Supporting Information. The prepared MSNs were systematically characterized. Particle size and morphology were confirmed with transmission electron microscopy (TEM) (**Figure 1**). Pristine MSNs appear around 100 nm in diameter, spherical in shape with slightly rough surface and a hexagonal pore arrangement. Amino-modified particles (MSN-A) show unchanged morphology and pore arrangement, confirming no pronounced change on shape

Prof. H. A Santos
Helsinki Institute of Life Science (HiLIFE)
University of Helsinki
Helsinki FI-00014, Finland
Prof. M. A. McGuckin
Faculty of Medicine
Dentistry and Health Sciences
the University of Melbourne
Melbourne VIC 3010, Australia

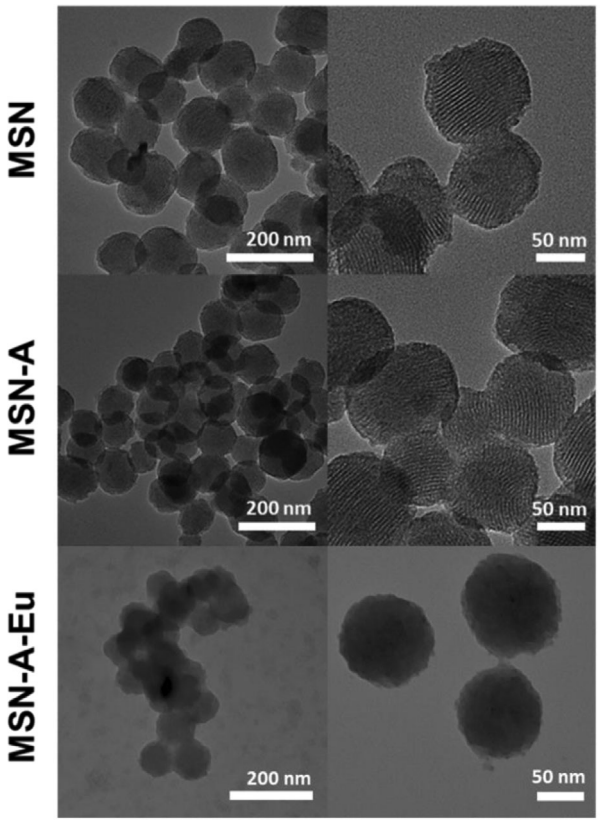

Figure 1. TEM images of pristine (MSN), amino-modified (MSN-A) and Eudragit S100 coated particles (MSN-A-Eu). Scale bars are 200 nm (left column) and 50 nm (right column).

Table 1. DLS particle size, surface charge and polydispersity index (PDI) of synthetized MSNs in pH 5.5 universal buffer. Data represent mean ± SD, (n=3).

	Size (number mean) [nm]	PDI	Surface charge [mV]
MSN	110.3 ± 4.3	0.16 ± 0.01	−13.5 ± 1.0
MSN-A	143.4 ± 3.7	0.11 ± 0.01	+33.6 ± 1.1
MSN-A-Pre	160.1 ± 14.6	0.21 ± 0.04	+30.2 ± 2.0
MSN-A-Bud	168.5 ± 10.8	0.26 ± 0.08	+29.8 ± 2.5
MSN-A-Eu	224.6 ± 15.0	0.41 ± 0.10	−20.9 ± 1.4
MSN-A-Eu-Pre	238.3 ± 12.7	0.42 ± 0.11	−19.2 ± 2.8
MSN-A-Eu-Bud	241.7 ± 18.6	0.45 ± 0.16	−19.5 ± 3.5

or the hexagonal structure after modification.[29] For coated particles, a layer of Eudragit S100 can be observed coated over the particles.

Particle size was measured by dynamic light scattering (DLS). Pristine MSNs show a hydrodynamic diameter of ≈110 nm, which increased to ≈143 nm for MSN-A (**Table 1**). Drug-loaded particles show slightly larger diameter (≈160 nm for MSN-A-Pre and ≈168 nm for MSN-A-Bud), which could be a result of increased hydrophobicity from drug loading on the porous surface of the nanoparticles. Hydrodynamic diameter further increases to ≈225 nm (MSN-A-Eu) after coating. Coated particles with drug show the size of ≈238 nm (MSN-A-Pre-Eu) and ≈242 nm (MSN-A-Bud-Eu). Zeta-potential of synthetized MSNs was measured in pH 5.5 universal buffer to confirm amino group modification and Eudragit S100 coating. The pristine particles show a negative zeta-potential of −13.5 mV, which is reversed to +33.6 mV because of amino groups after modification. Particles show slightly lower zeta-potential after drug loading (+30.2 mV for MSN-A-Pre and +29.8 mV for MSN-A-Bud). After coating MSN-A-Eu shows negative charge of -20.9 mV, as positively charged amino groups are covered by Eudragit S100. Coated particles loaded with drug have zeta-potential of −19.2 ± 2.8 mV (MSN-A-Pre-Eu) and −19.5 ± 3.5 mV (MSN-A-Bud-Eu) confirming successful coating of negatively charged Eudragit onto positively charged particles.

Table 2. Surface area and porosity of synthetized MSNs. Data represent mean ± SD, (n=3).

	BET surface area [$m^2\ g^{-1}$]	Pore volume [$cm^3\ g^{-1}$]	Pore size [nm]
MSN	5 0 ± 30	1.1 ± 0.02	2.1 ± 0.02
MSN-A	4 9 ± 15	1.0 ± 0.03	2.0 ± 0.01
MSN-A-Pre	2 1 ± 7	0.5 ± 0.02	N/A
MSN-A-Bud	3 5 ± 11	0.7 ± 0.02	N/A
MSN-A-Eu	2 4 ± 14	0.5 ± 0.01	N/A
MSN-A-Pre-Eu	2 6 ± 12	0.4 ± 0.02	N/A
MSN-A-Bud-Eu	2 0 ± 14	0.5 ± 0.02	N/A

Surface area and pore size distribution were analyzed by nitrogen (N_2) adsorption–desorption isotherm measurements. Pristine (MSN) and amino-modified particles (MSN-A) exhibit IUPAC type-IV isotherms according to N_2 adsorption–desorption analysis, affirming the mesoporous nature of the prepared MSN (**Figure 2**a). A steep capillary condensation step can be observed from these two samples between relative pressure (P/Po) of 0.2 and 0.4, indicating MSN and MSN-A have unchanged pore structure after amino modification. Pristine particles have a (Brunauer–Emmett–Teller) BET surface area of 550 $m^2\ g^{-1}$ (**Table 2**). MSN-A shows reduced BET surface area (489 $m^2\ g^{-1}$) because of binding of amino silane. After drug loading, the surface area of particles further decreases to 231 $m^2\ g^{-1}$ (MSN-A-Pre) and 345 $m^2\ g^{-1}$ (MSN-A-Bud), as pore volume is occupied by prednisolone and budesonide respectively. Eudragit S100 coated particles (MSN-A-Eu) shows even lower surface area of 241 $m^2\ g^{-1}$ because of the coverage of polymer chain. Surface area of MSN-A-Pre-Eu and MSN-A-Bud-Eu further drop to 226 and 220 $m^2\ g^{-1}$. The N_2 adsorption-desorption isotherm measurements confirmed that mesoporous pore structure of MSN-A-Eu was blocked, indicating the successful coating. Reduced pore size of MSN-A (2.0 nm) compared to MSN (2.2 nm) comes from introduced amino silane (Figure 2). Similarly, pore volume of particles reduced from 1.20 to 0.99 $cm^3\ g^{-1}$ after amino modification. MSN-A-Pre, MSN-A-Bud, and MSN-A-Eu showed pore volume of 0.48, 0.54, and 0.51 $cm^3\ g^{-1}$. Coated particles with drug showed lowest pore volume of 0.16 $cm^3\ g^{-1}$ (MSN-A-Pre-Eu) and 0.19 $cm^3\ g^{-1}$ (MSN-A-Bud-Eu).

Loading percentage (w/w) of prednisolone is 16.8% and 29.2% for particles with (MSN-A-Pre-Eu) and without (MSN-A-Pre) coating, respectively, with loading efficiency of 95.2% and 97.3%.

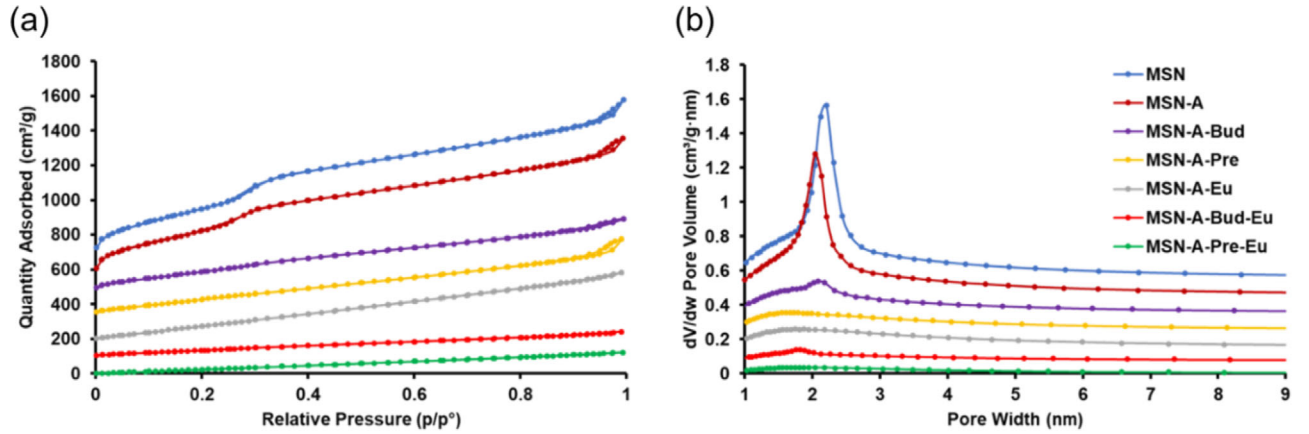

Figure 2. a) N_2 adsorption/desorption isotherms and b) pore size distributions (Barrett–Joyner–Halenda Adsorption dV/dD Pore Volume) of MSN, MSN-A, and MSN-A loaded with budesonide/prednisolone (MSN-A-Bud/MSN-A-Pre), particles with Eudragit S100 coating (MSN-A-Eu), and drug loaded particles with Eudragit S100 coating (MSN-A-Bud-Eu/MSN-A-Pre-Eu).

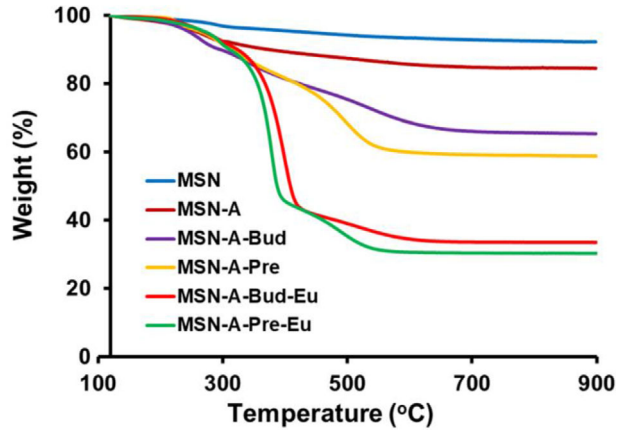

Figure 3. Weight loss profile of MSN, MSN-A, and MSN-A loaded with budesonide/prednisolone (MSN-A-Bud/MSN-A-Pre) and drug loaded nanoparticles with Eudragit S100 coating (MSN-A-Bud-Eu/MSN-A-Pre-Eu) determined by TGA from 100 to 900 °C.

For budesonide, loading percentage (w/w) was 9.0% for MSN-A-Bud-Eu and 19.1% for MSA-A-Bud with 82.0% and 95.5% loading efficiency. Loading of prednisolone and budesonide were quantified via UV visible for prednisolone and using HPLC for budesonide. Drug loading was further confirmed with thermogravimetric analysis (TGA) (**Figure 3**). Weight losses were determined by computed as functions of temperature in comparison to respective control. Weight loss was calculated from 120 °C to exclude weight loss from moisture. MSN-A appears 15.4% weight loss, which is 7.7% higher than that of pristine particles, confirming success of amino modification. Further weight loss observed in MSN-A-Pre and MSN-A-Bud comes from loaded prednisolone and budesonide. MSN-A-Pre-Eu and MSN-A-Bud-Eu appear to have the most weight loss because of Eudragit coating.

Wide angle X-ray diffraction (WXRD) was performed to confirm the nature of encapsulated prednisolone and budesonide within mesopores of MSN. The WXRD spectrum between a 2θ ranges of 10° to 40° were obtained for MSN with and without loading (**Figure 4**). Pure prednisolone and budesonide show multiple sharp diffractions peaks from 10° to 30°, corresponding to lattice orientations from crystalline molecule. The amorphous nature of MSN-A and Eudragit S100 is evidenced by the absence of sharp peaks from 10° to 40°.[30] The diffraction peaks corresponding to free drugs can still be observed in drug-loaded MSN (i.e., MSN-A-Pre and MSN-A-Bud), indicating limited crystalline state of loaded drug. Interestingly, for MSN-A-Bud, although most of the diffraction peaks corresponding to budesonide are not as sharp as free budesonide, a very sharp peak is observed at 12°. However, for the drug loaded nanoparticles with Eudragit S100 coating, no diffraction peaks originating from crystalline drug was observed, suggesting that loaded drug is entrapped within MSN-A and polymer nanocomposites in an amorphous form.[30]

2.2. In Vitro Release of Fabricated pH-Responsive Nanoparticles

The pH-responsive in vitro release was studied by suspending the drug-loaded particles in pH 1.9 aqueous buffer solutions (universal buffer according to USP). At 2 and 5 h time points, the pH of the buffer was adjusted to 5.5 and 7.4, respectively, to mimic the progressive pH environments of the GIT. Free prednisolone shows burst release of around 86% in the first 2 h at pH 1.9. Similar release profile was observed for MSN-A-Pre with 76% release (**Figure 5**a) in the first 2 h. However, MSN-A-Pre-Eu showed only 18% drug release in the first 2 h (pH 1.9) and additional 10% released between 2 and 5 h (pH 5.5), followed by up to 78% release over 24 h after the pH was adjusted to 7.4. For budesonide, free drug was released up to 56% in the first 2 h, followed by 71% release in 24 h. Compared to prednisolone, budesonide shows limited dissolution, which is because of its poor aqueous solubility. The release of MSN-A-Bud followed similar trend to free budesonide with around 80% budesonide release in first 5 h (Figure 5b). The pH-responsive release was also observed from MSN-A-Bud-Eu with only 12% release at pH 1.9 and another 7% release at pH 5.5. Approximately 60% loaded budesonide was released only after pH was adjusted to 7.4 consistent with MSN-A-Pre-Eu.

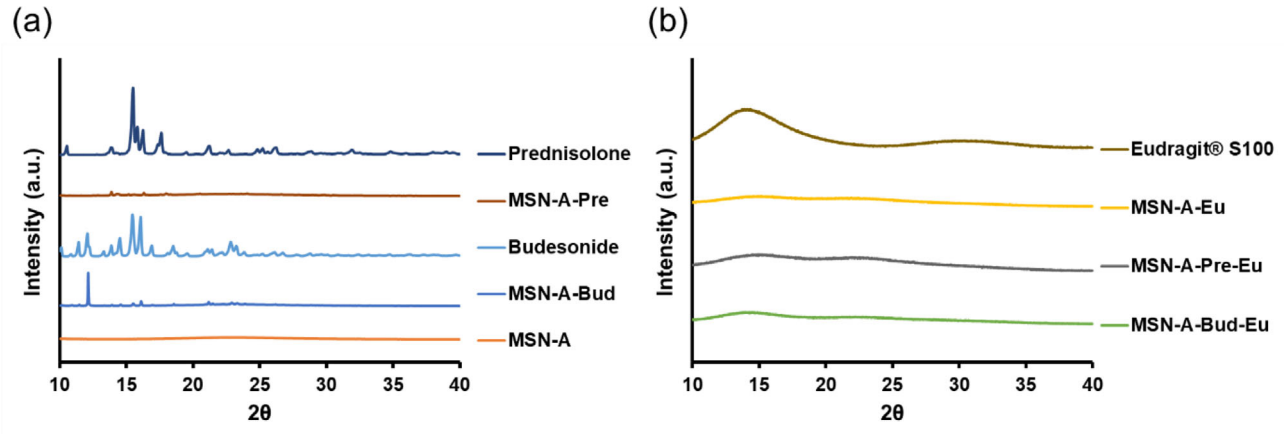

Figure 4. Wide angle X-ray diffractograms (WXRD) patterns of a) free drug and drug-loaded silica nanoparticles, b) free polymer (Eudragit S100) and coated and drug-loaded nanoparticles.

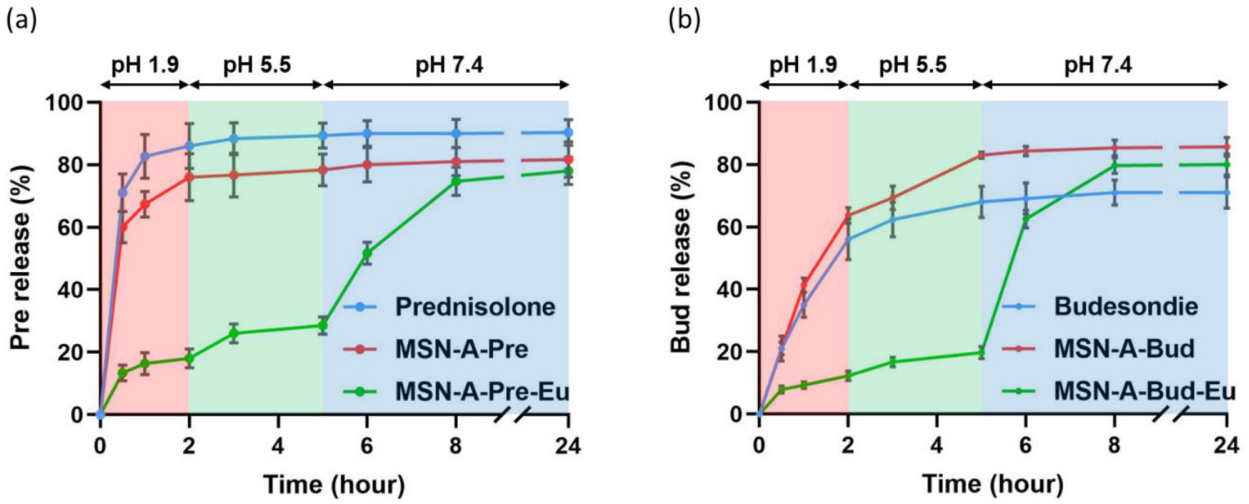

Figure 5. a) Cumulative release profile of prednisolone and b) budesonide from free drug, particles with and without coating exposed in universal buffers at 37 °C. Release was started at pH 1.9 for the first 2 h. Then pH was adjusted to 5.5 for 3 h. At last, pH was adjusted to 7.4 till end of release. Data represent mean ± SD, ($n = 3$).

Therefore, for both drugs, loading and Eudragit S100 coating provides protection from acidic pH, leading to potentially promising pH-responsive drug delivery for IBD.[14]

2.3. In Vivo Efficacy Against DSS-Induced Colitis

The therapeutic efficacy of budesonide encapsulated in Eudragit S100 coated silica nanoparticles in the DSS-induced colitis model was investigated because of the known anti-inflammatory properties of budesonide in this model.[31] DSS directly damages the intestinal lining allowing luminal content to come in direct contact with the epithelium. These results in immune activation in the intestinal epithelium, immune cell infiltration, and subsequent epithelial inflammation.[28] These made DSS model one of the most widely used murine models due to its simplicity, rapidity, controllability, reproducibility, and resemblance to human ulcerative colitis.[32]

We scored the animals for disease severity in terms of diarrhea score and rectal bleeding, which were cumulatively represented as DAI score in **Figure 6**a (Histology scoring sheet DSS colitis, Supporting Information). The result showed that all treatment groups improved DAI score compared to DSS colitis group, especially MSN-A-Bud and MSN-A-Bud-Eu (Figure 6a). DSS caused significant body weight loss, increased colon weight, decreased length, and increased weight–length ratio (Figure 6b–e). However, no significant improvement of colon weight or length was observed in the treatment groups. We also measured histological colitis by scoring the hematoxylin and eosin (H&E)-stained sections. As expected, DSS colitis group had highest histological score confirming inflammation. Representative images from each group and blind assessment of histological colitis, are shown in **Figure 7**. In the proximal colon, preservation of epithelial cells can be observed in all treatment groups, including free budesonide group, compared to DSS colitis group (Figure 7). Interestingly, MSN-Bud showed reduced histological colitis score

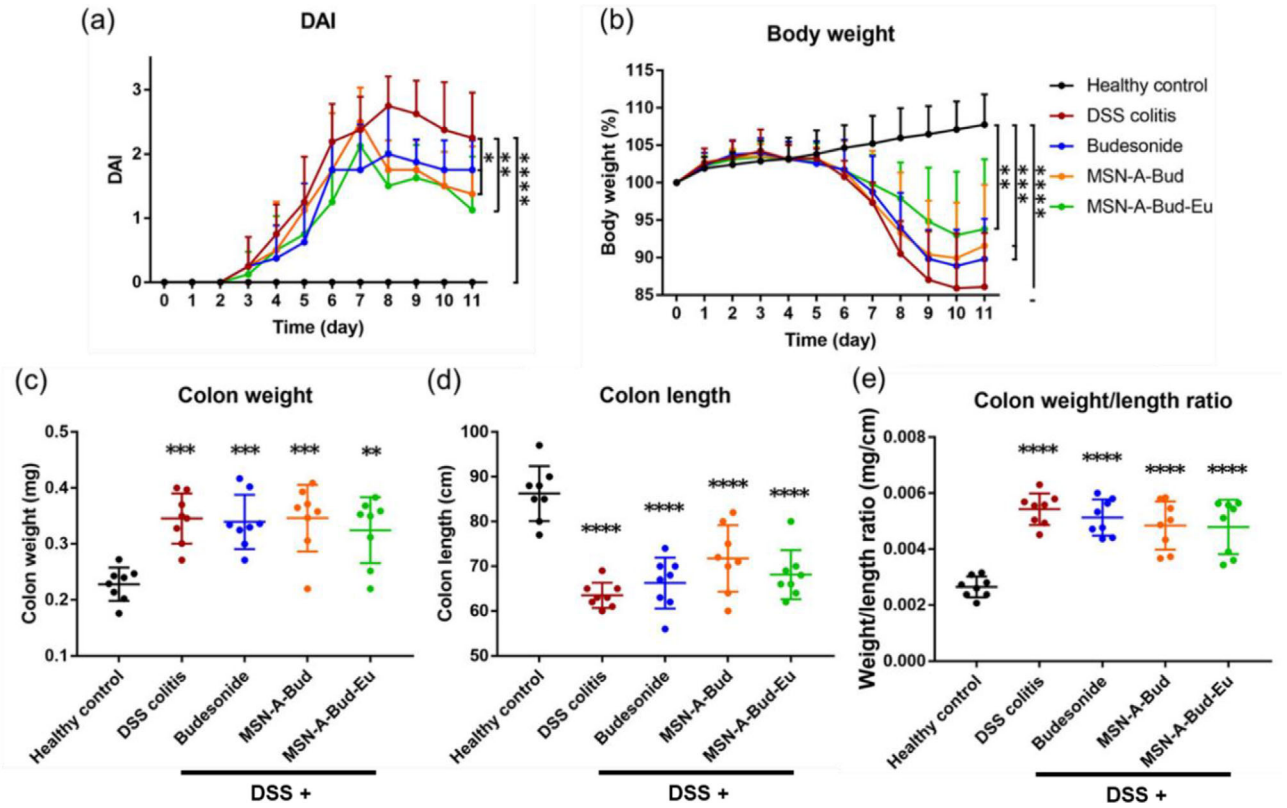

Figure 6. Therapeutic efficacy of budesonide dosages on IBD model of DSS-induced colitis in mice. For treatment groups, 0.2 mg kg^{-1} budesonide and equivalent dose loaded particles were given via oral gavage in PBS daily from day 7 to day 11. Colon tissues were collected and measured after sacrifice on day 12. PBS or particles without loading in PBS were given to the control group via oral gavage at same time point. Data were collected from 4 mice per group in two independent experiments. a) DAI (disease activity index: diarrhea + rectal bleeding): $*p < 0.05$, $**p < 0.01$, and $****p < 0.0001$, compared to DSS colitis group; b) body weight normalized as percentage of initial body weight; c) colon weight, d) length, and e) colon weight/length ratio. $**p < 0.01$, $***p < 0.001$, and $****p < 0.0001$, compared to healthy control. DAI and body weight were analyzed by two-way ANOVA. Colon weight, length, and weight/length ratio were analyzed by one-way ANOVA (Dunnett's multiple comparisons test). Data are presented as mean ± SD ($n = 8$).

similar to MSN-A-Bud-Eu. It is possible that because of the pH and composition differences between healthy and inflammatory condition, the release of budesonide from the nanoparticles was slower than that observed in vitro. This may also be the reason that encapsulated budesonide did not show superior therapeutic effect in the proximal colon compared to free drug. Preservation of goblet cells and crypt structures can be observed in MSN-Bud and MSN-A-Bud-Eu groups (**Figure 8**). Similarly, free budesonide also showed improvement in histological colitis in the distal colon. The results of distal colon indicate higher delivery efficiency of nanoparticles to the distal colon compared to proximal colon. However, both nanoparticle groups loaded with budesonide (MSN-Bud, MSN-A-Bud-Eu) showed significantly reduced histological damage compared to DSS colitis group and free budesonide (Figures 7 and 8). This can be a result of incomplete dissociation of coated Eudragit S100 from decreased pH values from inflammation in the intestinal tract,[33] and possible variation in colonic pH between human and mice, which will need to be further investigated via pharmacokinetic studies. Pharmacokinetic study is another potential way to differentiate between different formulations and pure drug however due to very low dose of Budesonide (0.2 mg kg^{-1}) used in the study it is very difficult to perform PK in mice as seen with many recent studies using budesonide for the treatment of IBD.[13d,20c,21b,22c,34] Therefore, in order to assess the ability of coated particles to deliver budesonide more effectively, we decided to perform qRT PCR of the colonic tissues in order to prove local delivery and to study the expression of pro-inflammatory cytokines with different treatment groups. Corroborating previous studies, we observed an elevation in the levels of pro-inflammatory cytokines including *Il-1β, Il-17, and Tnf-α* (**Figure 9**).[35] Although we did not observe any changes in the gene expression with free budesonide, oral delivery using MSN-loaded budesonide and Eudragit coated nanoparticles (MSN-A-Bud-Eu) enhanced the anti-inflammatory activities of budesonide through reduction of *Il-1β* ($p < 0.05$ and $p < 0.01$, respectively) and *Il-17* ($p < 0.01$) in the proximal site (Figure 9a,b). These can be supported by a study from Djaldetti and Bessler,[35h] who showed budesonide reduces production of IL-1β in the peripheral blood mononuclear cells (PBMCs). We also observed a trend of reduced *Il-1β* and *Il-17* in the distal site (Figure 9d,e); however, no changes were found in the expression of *Tnf-α* (Figure S7, Supporting Information). Immunoregulatory cytokines such as Il-10 have shown to be elevated during intestinal inflammation, which decline after successful treatment.[35e] Interestingly, Eudragit-coated nanoparticle with budesonide significantly reduced the *Il-10*

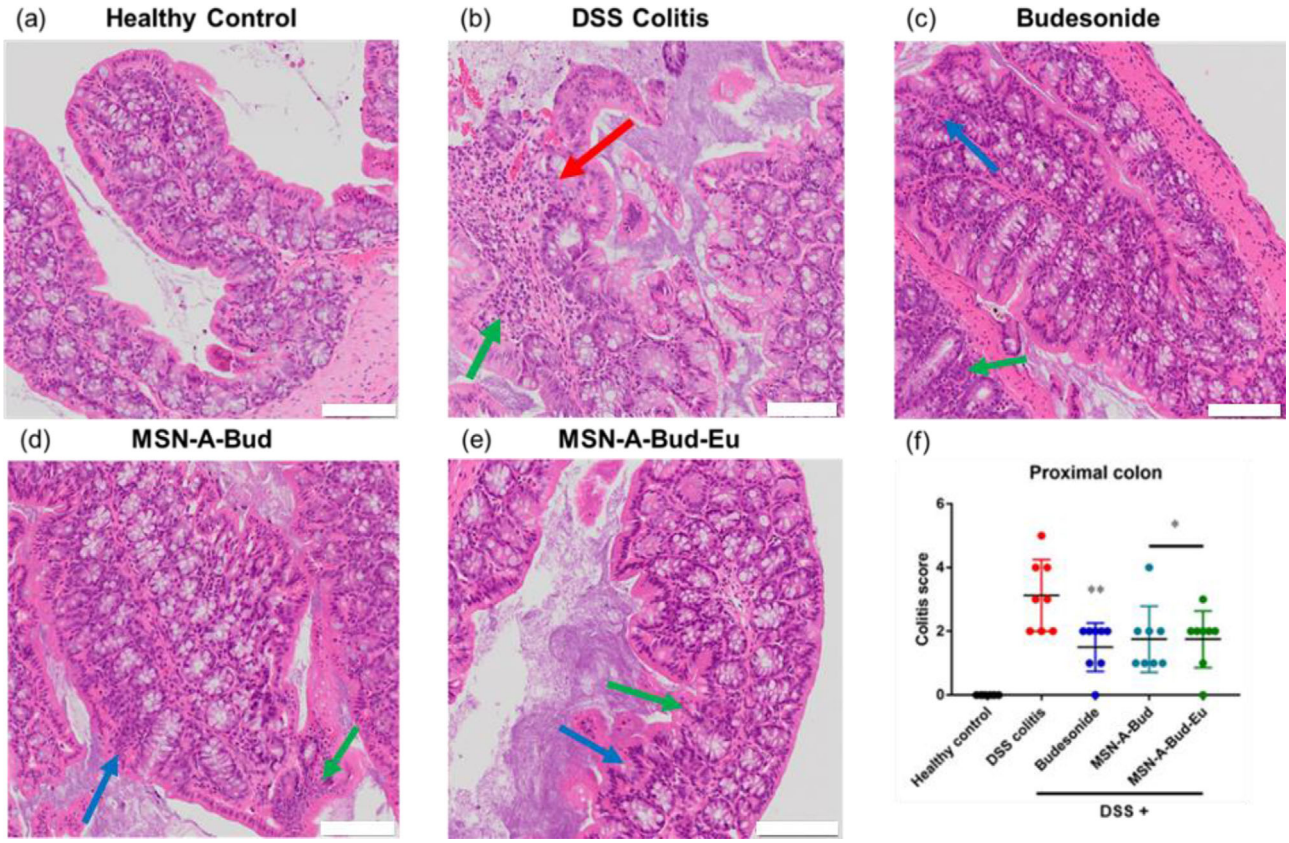

Figure 7. Therapeutic efficacy of free and MSN formulated budesonide on IBD model of DSS-induced colitis on mice. Representative histology images of H&E stained proximal colon sections from a) healthy control, b) DSS colitis, c) budesonide, d) MSN-A-Bud, e) MSN-A-Bud-Eu, and f) colitis score. Histological colitis was assessed based on inflammation severity (IS), infiltration extent (IE), epithelial damage (ED), and percentage involvement of epithelial damage (PD) (crypt abscessed, crypt loss, or ulceration). Data was analyzed by one-way ANOVA. $*p < 0.05$ and $**p < 0.01$, compared to DSS colitis group. (one-way ANOVA followed by Dunnett's multiple comparisons test). Data are presented as means ± SD ($n = 8$). Scale bars = 100 µm. Red arrows indicate crypt loss and abscesses, blue arrows represent goblet cell damage, and green arrows represent neutrophil infiltration.

expression compared to DSS group, suggesting that there was an overall reduction in inflammation in the intestine (Figure 9c,f). Djaldetti and Bessler have shown that budesonide also reduced the production of IL-10 in the LPS-stimulated PBMCs.[35h] Gene transfer[35a] or administration of IL-10[36] was also shown to suppress experimental colitis, whereas deficiency of IL-10 led to the development of colitis,[35b] demonstrating a protective role of this cytokine to maintain intestinal homeostasis. IL-10 was found to down-regulate expression of IL-1β in the monocytes from colitis patients,[35d] which could be correlated with the reduced expression of *Il-1β* in our experiment. Moreover, IL-10 was also shown to suppress Th17 immune responses and reduce expression of pro-inflammatory cytokine IL-17.[35g] As immune cells express IL-10 receptors, these indicate that increased expression of IL-10 may produce an anti-inflammatory environment in the colon by educating the infiltrated immune cells. It has also been found that controlling an autoregulative negative feedback mechanism, IL-10 can reduce its own synthesis in monocytes.[35c] Besides, budesonide also reduced immune cell infiltration in the inflamed colon (Figures 7 and 8). Therefore, it is possible that reduced inflammatory state created by budesonide also impacted on the observed level of *Il-10* expression with nanoparticles treated colon. It is important to note that when compared to budesonide only coated particles, (MSN-A-Bud-Eu) reduced *Il-10* expression in the distal colon further attesting improved colonic delivery with coated particles. Overall, these results demonstrated that encapsulation of budesonide increased its therapeutic efficiency, and pH-responsive Eudragit coating further enhanced the activity with less body weight loss, less DAI and histological colitis scores, and decreased expression of pro-inflammatory cytokines in the DSS-treated animals. These data therefore supported the effectiveness of budesonide nanoformulation in ulcerative colitis. The limited recovery from free budesonide could be because the severity of inflammation was beyond efficacy of selected dose of budesonide. The observed beneficial effects of encapsulated budesonide could be the result of site-specific release of budesonide at the colonic site.

3. Conclusion

In this study, a colon targeting oral drug delivery system based on mesoporous silica nanoparticles and Eudragit S100 was developed and optimized. Prepared silica nanoparticles ≈150 nm in size have well-defined spherical morphology and ordered mesoporous structure. The encapsulation of drug and pH-responsive polymer coating were achieved with a one-step rotary evaporation

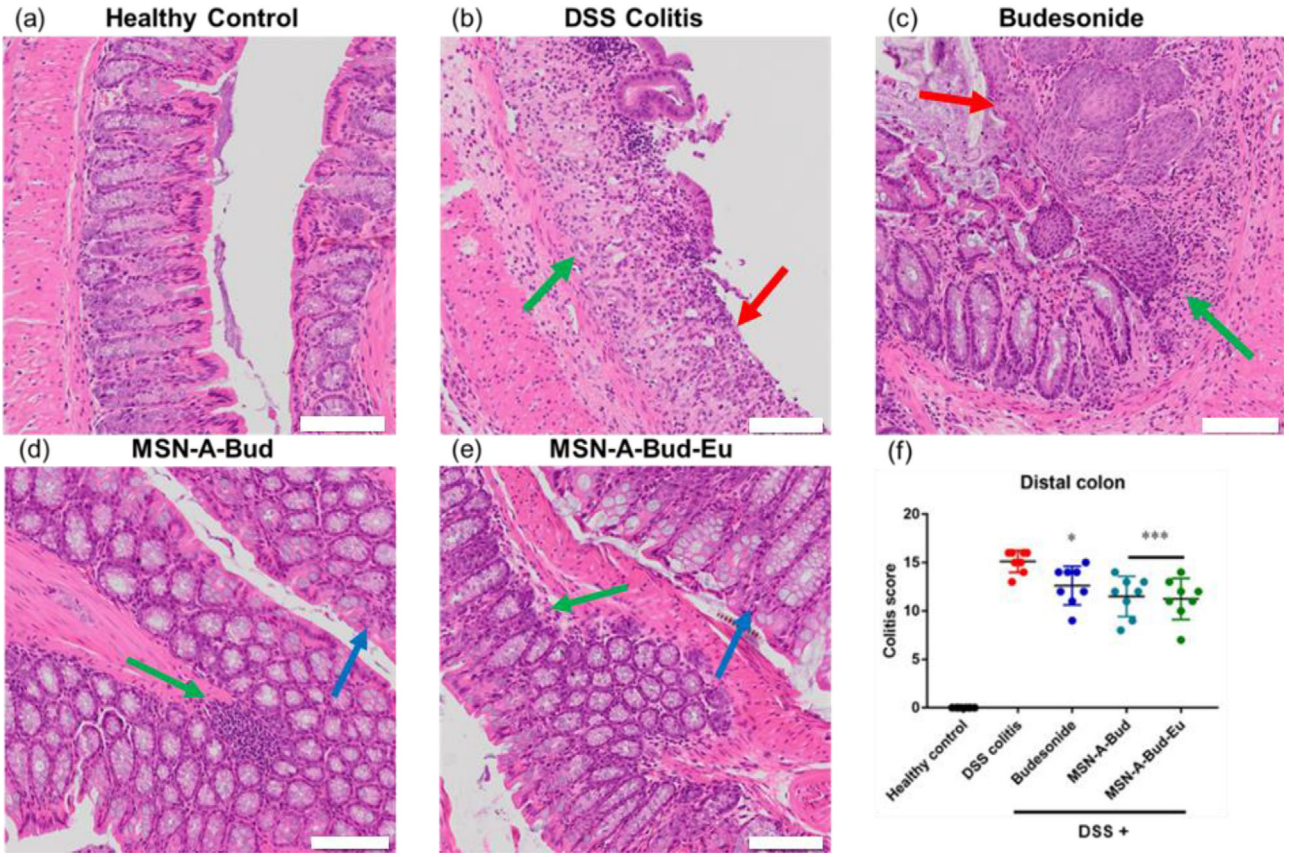

Figure 8. Therapeutic efficacy of free and MSN-formulated budesonide on IBD model of DSS-induced colitis on mice. Representative histology images of H&E stained distal colon sections from a) healthy control, b) DSS colitis, c) budesonide, d) MSN-A-Bud, e) MSN-A-Bud-Eu, and f) colitis score. Histological colitis was assessed based on IS, IE, ED, and PD. Data was analyzed by one-way ANOVA. $*p < 0.05$ and $***p < 0.001$, compared to DSS colitis group (one-way ANOVA followed by Dunnett's multiple comparisons test). Data are presented as means ± SD ($n = 8$). Scale bars = 100 µm. Red arrows indicate crypt loss and abscesses, blue arrows represent goblet cell damage, and green arrows represent neutrophil infiltration.

method. Corticosteroid drugs prednisolone (16.8% w/w) and budesonide (9.0% w/w) were successfully encapsulated and coated with Eudragit S100 onto synthesized particles. The polymer coating with Eudragit S100 protected the loaded drugs against the acidic condition of GIT before reaching colonic site, and prevented premature release of both prednisolone and budesonide. The therapeutic effect of budesonide was also tested using a murine model of DSS-induced colitis. Encapsulation of budesonide within MSN significantly reduced inflammation compared to free drug via significant improvement in DAI and histological lesion score, especially in the distal colon. Although we did not find significant difference between coated and uncoated particles in improving histology, coated nanoparticles effectively alleviated the DSS-induced upregulation of cytokines *Il-1β*, *Il-10*, and *Il-17* compared to uncoated particles in the proximal colon and *Il-10* in the distal colon. Overall, the design of pH-responsive mesoporous silica nanoparticles is promising as a new cost-efficient oral delivery system for better IBD treatment. Our future work will focus on assessing in vivo pharmacokinetics of the released drug and delineating the role of particle accumulation on improvement of disease pathology with and without pH-responsive coating.

4. Experimental Section

Materials: 99% Tetraethylorthosilicate (TEOS), 99% hexadecyltrimethylammonium bromide (CTAB), 99% (3-aminopropyl) triethoxysilane (APTES), and 99% prednisolone were purchased from Sigma-Aldrich, St Louis, MO, USA. Ethanol, methanol, chloroform, and 32% hydrochloric acid was purchased from Merck KGaA, Darmstadt, Germany. Phosphoric acid (H_3PO_4), acetic acid (CH_3COOH), and sodium hydroxide were purchased from Chem-Supply, Gillman, SA, Australia. Budesonide was purchased from BioNet, Camelford, UK. Dextran sodium sulfate (MW 36–50 kDa) was purchased from MP Biochemicals, Illkirch, France. Eudragit S100 was a generous gift from Evonik, Germany. Phosphate-buffered saline tablets were purchased from MP Biomedicals, Santa Ana, CA, USA. ISOLATE II RNA Mini Kit (BIOLINE, Australia), and SensiFAST cDNA synthesis kit (BIOLINE, Australia) were used as directed by the manufacturer.

Synthesis of Mesoporous Silica Nanoparticles: Mesoporous silica nanoparticles were synthesized according to a previously reported method with specific modification.[37] Briefly, 1.0 g of CTAB was added in 480 mL of deionized (DI) water at ambient temperature, followed by addition of 3.5 mL of 2 M of NaOH and heated to 80 °C. The mixture was stirred for 2 h after adding 6.7 mL of TEOS. The resultant suspension was vacuum filtered and washed by DI water and ethanol. Washed particles were dried overnight at 60 °C and kept for further experiment. Surfactant was removed by solvent extraction, according to the reported protocol with slight modifications.[38] For this, 0.6 g of particles were dispersed in 64 mL

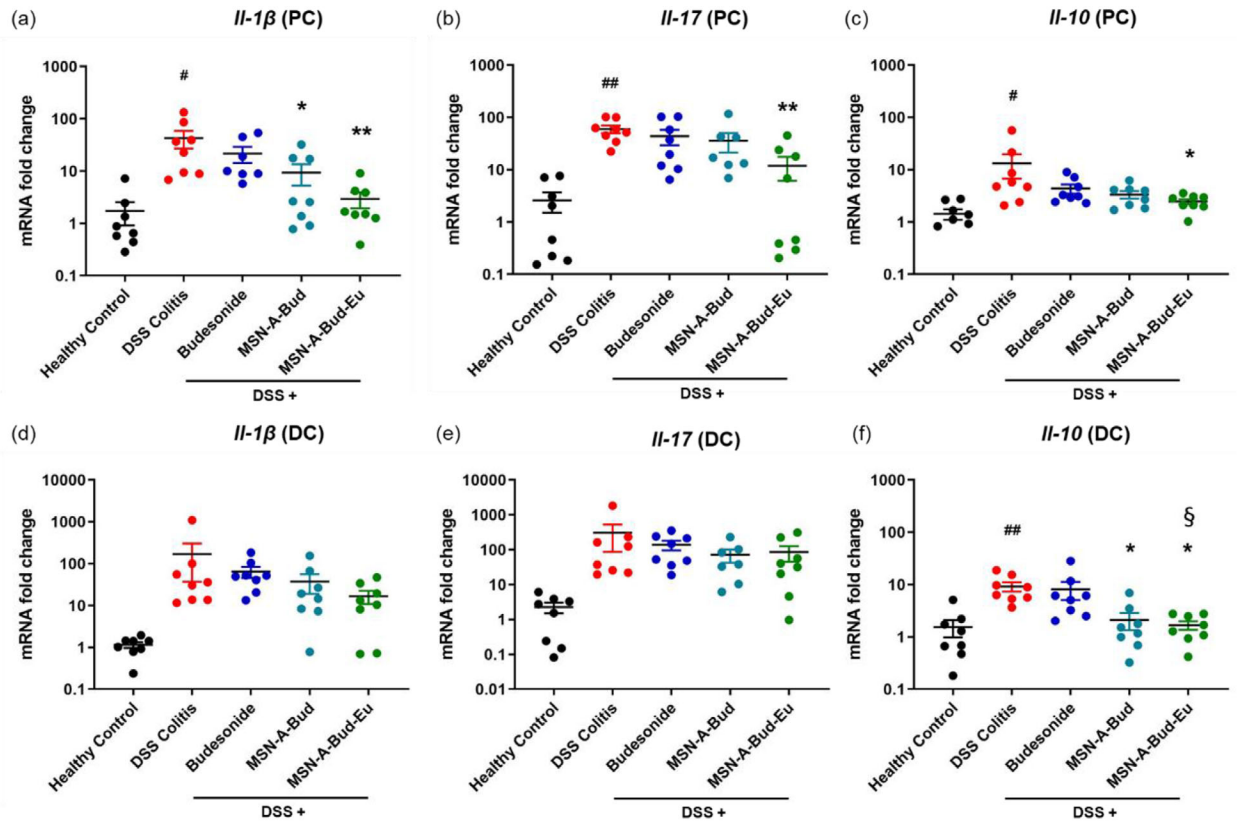

Figure 9. Gene expression of *Il-1β*, *Il-17 and Il-10* in the proximal (a–c) and distal (d–f) colon were determined by qRT-PCR. *Tata box* was used as a housekeeping gene. Expression level was normalized to healthy control. Data are presented as mean ± SEM ($n = 8$), § $p < 0.05$ compared with budesonide group, * $p < 0.05$; ** $p < 0.01$ compared with DSS group and # $p < 0.05$; ## $p < 0.01$ compared with control group (one-way ANOVA followed by Dunnett's multiple comparisons test).

of ethanol and 4.0 mL of hydrochloric acid (32%) and stirred at 60 °C for 36 h. Particles were retrieved by centrifugation at 20 000 *g* for 10 min and washed with DI water and ethanol. Washed particles were dried overnight and denoted as MSN for further studies.

Amino Functionalization of Mesoporous Silica Nanoparticles: Amino-functionalized MSNs were prepared according to previously reported method with slight changes.[39] Functionalization was processed before surfactant removal to avoid blockage of pore entrance. Briefly, 0.8 g of MSNs without surfactant removal was dispersed in 50 mL of methanol. After adding 3.0 mL of APTES, the mixture was stirred at room temperature overnight. Modified particles were retrieved and washed by centrifugation and dried overnight. Solvent extraction was carried out after functionalization as described above. Prepared particles were noted as MSN-A.

Eudragit S100 Coating and Drug Loading: Eudragit S100 coated MSN-A loaded with prednisolone was prepared with rotary evaporation method. 30 mg of prednisolone was dissolved in 1 mL of methanol. 70 mg of MSN-A was dispersed in another 1 mL of methanol and mixed with 1 mL of methanol with prednisolone. Next, 70 mg of Eudragit S100 was dissolved in another 2 mL of methanol and added into the suspension of MSN-A and prednisolone. Mixture was sonicated in water bath for 30 min. Methanol was then evaporated with a rotary evaporator at 40 °C. Collected particles were noted as MSN-A-Pre-Eu. Budesonide was loaded with same method with different ratio (20 mg budesonide/80 mg MSN-A/80 mg Eudragit S100) and noted as MSN-A-Bud-Eu. Please note that the Eudragit S100 coated particles without loading are denoted as MSN-A-Eu throughout the manuscript.

Characterization: TEM images were obtained with a Hitachi 7700 microscope operated at 80 kV. Particle size and zeta-potential of the prepared MSNs were measured with DLS setup (Malvern, Nano-ZS, ATA Scientific, Taren Point, Australia). Surface area and pore volume were measured with nitrogen absorption (N_2-BET), (Tristar 3020, Micromeritics-II, Norcross, GA, USA). WXRD was recorded on a Rigaku Miniflex X-ray diffractometer with Cu radiation ($k = 1.54$ Å). TGA was performed with a heating rate of 10 °C min^{-1} under ambient air (Mettler Toledo, TGA/DSC 2, Columbus, OH, USA). Drug content was quantified according to reported method.[40] Prednisolone was analyzed with Agilent Cary 60 UV–visible spectrophotometer at a wavelength of 250 nm. Budesonide was analyzed using HPLC (Nexera-I LC-2040 3D, Shimadzu, Japan) with an UV/visible detector at a wavelength of 254 nm and Luna C18 column (150 × 4.6 mm, 5 µm Phenomenex, USA), eluted with 70% v/v methanol in water at a flow rate of 1.5 mL min^{-1}. Loaded drug was quantified after extraction from particles with methanol. Loading percentage and efficiency of prednisolone and budesonide were calculated with the following equations:

$$\text{Loading percentage } (\%) = \frac{\text{Amount of drug loaded}}{\text{Total amount of MSNs and loaded drug}} \times 100\% \quad (1)$$

$$\text{Loading efficiency } (\%) = \frac{\text{Amount of drug loaded}}{\text{Total amount of drug initially used for loading}} \times 100\% \quad (2)$$

In Vitro pH-Responsive Drug Release: The pH-responsive drug release properties of the Eudragit S100 coated silica nanoparticles loaded with prednisolone and budesonide were elucidated using the "universal buffer," according to the United States Pharmacopeia (USP).[40a] Typically, 1 mg of drug and equivalent dose of drug-loaded particles were dispersed in 100 mL of universal buffer. Universal buffer was prepared by mixing 0.05 M of acetic acid and 0.05 M of phosphate buffer 1:1 by volume (pH 1.9). The pH of release media was adjusted to 5.5 and 7.4 with 8 M of NaOH at 2- and 5-h time points to mimic the progressive pH change of GIT. At specific time intervals, 2 mL of release media was collected and replaced with fresh release media. The collected release media was centrifuged at 20 000 *g* for 10 min to separate possible suspended nanoparticles, and the amount of drug in supernatant was quantified.

DSS-Induced Colitis Model: All animal research and experiment protocols were approved by the Animal Ethics Committee of the University of Queensland and conducted according to National Health and Medical Research Council guidelines. AEC Approval Number: PHARM/TRI/251/18.

The 6-week-old male C57BL/6J mice were obtained from Animal Resources Centre (ARC). Formulated drinking water with 1.5% DSS water was provided ad libitum from day 0 for 7 days. Normal drinking water was provided from day 7. The body weights of mice were monitored and recorded. Each mouse was examined daily to record the disease activity index (DAI). DAI is defined as the diarrhea score plus the rectal bleeding score. Details of scoring are listed below. For diarrhea and rectal bleeding scoring, 0 = normal/equivocal symptoms, 1 = mild symptoms, and 3 = severe symptoms. For weight loss scoring, 0 ≤ 5% weight loss, 1 = 5–14% weight loss, 2 = 15–19% weight loss, and 3 ≥ 20% weight loss (Supporting Information).[41]

For therapeutic efficacy experiment, 6-week-old male C57BL/6J mice were divided into seven groups ($n = 8$ per group). 0.2 mg kg^{-1} free budesonide and budesonide-encapsulated nanoparticles with equivalent dose were dispersed in PBS and given to the corresponding group via oral gavage daily from day 7 to day 11. Body weight and DAI were recorded daily. Animals were sacrificed on day 12. Colonic tissues were collected, cut longitudinally, with fecal material removed gently with a pipette tip and measured for weight and length. For histological assessment of DSS colitis, samples were fixed in formalin overnight. Fixed tissues were then dehydrated in ethanol overnight and embedded in paraffin. 5 µm sections of rolled colon tissue were cut and fixed on slides, stained with H&E. Stained slides were scanned and scored in blinded fashion, according to validated scoring system by inflammation severity, infiltration extent, epithelial damage, and percentage involvement of epithelial damage (crypt abscessed, crypt loss, or ulceration), using a well-developed scoring system.[42] Quantitative real time polymerase chain reaction (qRT-PCR) of colon tissue was processed with ISOLATE II RNA Mini Kit (Bioline), according to the manufacturer's instructions.

Supporting Information

Supporting Information is available from the Wiley Online Library or from the author.

Acknowledgements

The authors are thankful for research maintenance funds provided by the School of Pharmacy, The University of Queensland, and the funding provided by the Mater Medical Research Institute. A.P. and T.K. are thankful to the National Health and Medical Research Council of Australia for Career Development (GNT 1146627) and Early Career Fellowship (GNT1143296), respectively. The authors are also thankful to the Centre of Microscopy and Microanalysis (CMM) at UQ and TRI for providing facilities.

Conflict of Interest

The authors declare no conflict of interest.

Keywords

colitis, colonic delivery, Eudragit, MCM-41, mesoporous silica, oral drug delivery

Received: July 21, 2020
Revised: September 10, 2020
Published online:

[1] a) J. Burisch, T. Jess, M. Martinato, P. L. Lakatos, E. EpiCom, *J. Crohns Colitis* **2013**, *7*, 322; b) S. Z. Hasnain, R. Lourie, I. Das, A. C. H. Chen, M. A. McGuckin, *Nat. Publ. Group* **2012**, *90*, 260; c) S. Z. Hasnain, S. Tauro, I. Das, H. Tong, A. C. H. Chen, P. L. Jeffery, V. McDonald, T. H. Florin, M. A. McGuckin, *Gastroenterology* **2013**, *144*, 357.

[2] a) J. Wilson, C. Hair, R. Knight, A. Catto-Smith, S. Bell, M. Kamm, P. Desmond, J. McNeil, W. Connell, *Inflamm. Bowel Dis.* **2010**, *16*, 1550; b) O. Niewiadomski, C. Studd, C. Hair, J. Wilson, J. McNeill, R. Knight, E. Prewett, P. Dabkowski, D. Dowling, S. Alexander, B. Allen, M. Tacey, W. Connell, P. Desmond, S. Bell, *J. Crohns Colitis* **2015**, *9*, 988; c) A. H. Teruel, É. Pérez-Esteve, I. González-Álvarez, M. González-Álvarez, A. M. Costero, D. Ferri, P. Gaviña, V. Merino, R. Martínez-Máñez, F. Sancenón, *Mol. Pharmaceutics* **2019**, *16*, 2418; d) Y. H. Sheng, K. Y. Wong, I. Seim, R. Wang, Y. He, A. Wu, M. Patrick, R. Lourie, V. Schreiber, R. Giri, C. P. Ng, A. Popat, J. Hooper, G. Kijanka, T. H. Florin, J. Begun, K. J. Radford, S. Hasnain, M. A. McGuckin, *Oncogene 38*, 7294, **2019**, DOI: 10.1038/s41388-019-0951-y.

[3] Y. H. Sheng, S. Z. Hasnain, T. H. Florin, M. A. McGuckin, *J. Gastroenterol. Hepatol.* **2012**, *27*, 28.

[4] a) T. H. J. Florin, J. D. Wright, S. D. Jambhrunkar, M. G. Henman, A. Popat, *Drug Discovery Today* **2019**, *24*, 37; b) M. Aloi, F. Nuti, L. Stronati, S. Cucchiara, *Nat. Rev. Gastroenterol. Hepatol.* **2014**, *11*, 99.

[5] a) S. Keely, S. M. Ryan, D. M. Haddleton, A. Limer, G. Mantovani, E. P. Murphy, S. P. Colgan, D. J. Brayden, *J. Controlled Release* **2009**, *135*, 35; b) D. K. Podolsky, *J. Gastroenterol.* **2003**, *38*, 63.

[6] R. W. Summers, D. M. Switz, J. T. Sessions, Jr., J. M. Becktel, W. R. Best, F. Kern, Jr, J. W. Singleton, *Gastroenterology* **1979**, *77*, 847.

[7] G. R. Lichtenstein, M. T. Abreu, R. Cohen, W. Tremaine, American Gastroenterological Association, *Gastroenterology* **2006**, *130*, 940.

[8] a) H. Yokoyama, S. Takagi, S. Kuriyama, S. Takahashi, H. Takahashi, M. Iwabuchi, S. Takahashi, Y. Kinouchi, N. Hiwatashi, I. Tsuji, T. Shimosegawa, *Inflammatory Bowel Dis.* **2007**, *13*, 1115; b) I. Marietta, S. Shanika de, G. Subrata, *Can. J. Gastroenterol.* **2010**, *24*, 127.

[9] W. Kruis, G. Kiudelis, I. Racz, I. A. Gorelov, J. Pokrotnieks, M. Horynski, M. Batovsky, J. Kykal, S. Boehm, R. Greinwald, R. Mueller, O. D. S. G. International Salofalk, *Gut* **2009**, *58*, 233.

[10] M. Sandborn, *Am. J. Gastroenterol.* **2002**, *97*, 2939.

[11] a) S. B. Hanauer, M. Sparrow, *Curr. Opin. Invest. Drugs* **2004**, *5*, 1192; b) K. P. Steed, G. Hooper, N. Monti, M. Strolin Benedetti, G. Fornasini, I. R. Wilding, *J. Controlled Release* **1997**, *49*, 115.

[12] a) A. Lamprecht, *Curr. Drug Targets Inflammation Allergy* **2003**, *2*, 137; b) W. J. Sandborn, S. Travis, L. Moro, R. Jones, T. Gautille, R. Bagin, M. Huang, P. Yeung, E. D. Ballard, *Gastroenterology* **2012**, *143*, 1218; c) F. Varum, A. Cristina Freire, R. Bravo, A. W. Basit, *Int. J. Pharm.* **2020**, https://doi.org/10.1016/j.ijpharm.2020.119372.

[13] a) J. Song, Y. Wei, J. Hu, G. Liu, Z. Huang, S. Lin, F. Liu, Y. Mo, Y. Tu, M. Ou, *Chemistry* **2018**, *24*, 212; b) Y. Liu, W. Wang, J. Yang, C. Zhou, J. Sun, *Asian J. Pharm. Sci. 8*, **2013**, 159; c) I. Hofmeister, K. Landfester, A. Taden, *Macromolecules* **2014**, *47*, 5768; d) M. Naeem, M. Choi, J. Cao, Y. Lee, M. Ikram, S. Yoon, J. Lee, H. R. Moon, M. S. Kim, Y. Jung, J. W. Yoo, *Drug Des. Dev. Ther.* **2015**, *9*, 3789.

[14] L. Lu, G. Chen, Y. Qiu, M. Li, D. Liu, D. Hu, X. Gu, Z. Xiao, *Sci. Bull.* **2016**, *61*, 670.

[15] a) A. Ethirajan, K. Schoeller, A. Musyanovych, U. Ziener, K. Landfester, *Biomacromolecules* **2008**, *9*, 2383; b) J. Andrieu, N. Kotman, M. Maier, V. Mailander, W. S. Strauss, C. K. Weiss, K. Landfester, *Macromol. Rapid Commun.* **2012**, *33*, 248; c) B. Kang, T. Opatz, K. Landfester, F. R. Wurm, *Chem. Soc. Rev.* **2015**, *44*, 8301; d) A. Ethirajan, A. Musyanovych, A. Chuvilin, K. Landfester, *Macromol. Chem. Phys.* **2011**, *212*, 915; e) A. Musyanovych, J. Schmitz-Wienke, V. Mailander, P. Walther, K. Landfester, *Macromol. Biosci.* **2008**, *8*, 127; f) R. Penjweini, S. Deville, L. D'Olieslaeger, M. Berden, M. Ameloot, A. Ethirajan, *J. Controlled Release* **2015**, *218*, 82.

[16] a) B. Li, J. He, D. G. Evans, X. Duan, *Int. J. Pharm.* **2004**, *287*, 89; b) X. She, L. Chen, L. Velleman, C. Li, H. Zhu, C. He, T. Wang, S. Shigdar, W. Duan, L. Kong, *J. Colloid Interface Sci.* **2015**, *445*, 151.

[17] A. Lamprecht, U. Schäfer, C.-M. Lehr, *An Official Journal of the American Association of Pharmaceutical Scientists* **2001**, *18*, 788.

[18] a) A. Lamprecht, *Nat. Rev. Gastroenterol. Hepatol.* **2010**, *7*, 311; b) J. Youshia, A. Lamprecht, *Expert Opin. Drug Delivery* **2016**, *13*, 281.

[19] a) H. Schmitz, C. Barmeyer, M. Fromm, N. Runkel, H. D. Foss, C. J. Bentzel, E. O. Riecken, J. D. Schulzke, *Gastroenterology* **1999**, *116*, 301; b) S. H. Lee, *Intest. Res.* **2015**, *13*, 11.

[20] a) K. Tahara, S. Samura, K. Tsuji, H. Yamamoto, Y. Tsukada, Y. Bando, H. Tsujimoto, R. Morishita, Y. Kawashima, *Biomaterials* **2011**, *32*, 870; b) L. B. Vong, J. Mo, B. Abrahamsson, Y. Nagasaki, *J. Controlled Release* **2015**, *210*, 19; c) M. Naeem, J. Cao, M. Choi, W. Kim, H. Moon, B. Lee, M. S. Kim, Y. Jung, J. W. Yoo, *Int. J. Nanomed.* **2015**, *2015*, 4565; d) S. Hua, E. Marks, J. J. Schneider, S. Keely, *Nanomed.: Nanotechnol. Biol. Med.* **2015**, *11*, 1117.

[21] a) R. Coco, L. Plapied, V. Pourcelle, C. Jerome, D. J. Brayden, Y. J. Schneider, V. Preat, *Int. J. Pharm.* **2013**, *440*, 3; b) H. Ali, B. Weigmann, E. M. Collnot, S. A. Khan, M. Windbergs, C. M. Lehr, *Pharm. Res.* **2016**, *33*, 1085; c) S. Mura, J. Nicolas, P. Couvreur, *Nat. Mater.* **2013**, *12*, 991.

[22] a) A. Guha, N. Biswas, K. Bhattacharjee, P. Das, K. Kuotsu, *Curr. Drug Delivery* **2016**, *13*, 574; b) S. w. Song, K. Hidajat, S. Kawi, *Chem. Commun.* **2007**, 4396; c) W. Li, Y. Li, Z. Liu, N. Kerdsakundee, M. Zhang, F. Zhang, X. Liu, T. Bauleth-Ramos, W. Lian, E. Makila, M. Kemell, Y. Ding, B. Sarmento, R. Wiwattanapatapee, J. Salonen, H. Zhang, J. T. Hirvonen, D. Liu, X. Deng, H. A. Santos, *Biomaterials* **2018**, *185*, 322.

[23] a) F. Caruso, R. A. Caruso, H. Mohwald, *Science* **1998**, *282*, 1111; b) C. T. Kresge, M. E. Leonowicz, W. J. Roth, J. C. Vartuli, J. S. Beck, *Nature* **1992**, *359*, 710; c) J. S. Beck, J. C. Vartuli, W. J. Roth, M. E. Leonowicz, C. T. Kresge, K. D. Schmitt, C. T. W. Chu, D. H. Olson, E. W. Sheppard, S. B. McCullen, J. B. Higgins, J. L. Schlenker, *J. Am. Chem. Soc.* **1992**, *114*, 10834; d) M. M. Abeer, A. K. Meka, N. Pujara, T. Kumeria, E. Strounina, R. Nunes, A. Costa, B. Sarmento, S. Z. Hasnain, B. P. Ross, A. Popat, *Pharmaceutics* **2019**, *11*, 418; e) Z. Chaudhary, S. Subramaniam, G. Khan, M. M. Abeer, Z. Qu, T. Janjua, T. Kumeria, J. Batra, A. Popat, *Front. Bioeng. Biotechnol.* **2019**, *7*, 225; f) T. Limnell, H. A. Santos, E. Mäkilä, T. Heikkilä, J. Salonen, D. Y. Murzin, N. Kumar, T. Laaksonen, L. Peltonen, J. Hirvonen, *J. Pharm. Sci.* **2011**, *100*, 3294.

[24] a) J. Liu, T. Liu, J. Pan, S. M. Liu, G. Lu, *Ann. Rev. Chem. Biomol. Eng.* **2018**, *9*, 389; b) K. Möller, T. Bein, *Chem. Mater.* **2017**, *29*, 371; c) C. F. Wang, M. P. Sarparanta, E. M. Makila, M. L. Hyvonen, P. M. Laakkonen, J. J. Salonen, J. T. Hirvonen, A. J. Airaksinen, H. A. Santos, *Biomaterials* **2015**, *48*, 108; d) C. A. McCarthy, W. Faisal, A. Apos, J. P. Shea, C. Murphy, R. J. Ahern, K. B. Ryan, B. T. Griffin, A. M. Crean, *J. Controlled Release* **2017**, *250*, 86; e) Y. Niut, A. Popatt, M. Yu, S. Karmakar, W. Gu, C. Yu, *Ther. Delivery* **2012**, *3*, 1217; f) E. Juère, F. Kleitz, *Microporous Mesoporous Mater.* **2018**, *270*, 109; g) Z. Chaudhary, G. M. Khan, M. M. Abeer, N. Pujara, B. Wan-Chi Tse, M. A. McGuckin, A. Popat, T. Kumeria, *Biomater. Sci.* **2019**, *7*, 5002, DOI: 10.1039/c9bm00822e.

[25] a) J. M. Rosenholm, M. Lindén, *J. Controlled Release* **2008**, *128*, 157; b) I. S. Igor, L. V.-E. Juan, W. Chia-Wen, S. Y. L. Victor, *Adv. Drug Delivery Rev.* **2008**, *60*, 1278; c) N. Tyagi, R. De, J. Begun, A. Popat, *Int. J. Pharm.* **2017**, *518*, 220.

[26] a) E. V. Parfenyuk, *Silica Nanoparticles as Drug Delivery System for Immunomodulator GMDP*, ASME, New York **2012**; b) L. Li, T. Liu, C. Fu, L. Tan, X. Meng, H. Liu, *Nanomedicine* **2015**, *11*, 1915.

[27] a) J. Lu, Z. Li, J. I. Zink, F. Tamanoi, *Nanomed. Nanotechnol. Biol. Med.* **2012**, *8*, 212; b) M. Xie, H. Shi, Z. Li, H. Shen, K. Ma, B. Li, S. Shen, Y. Jin, *Colloids Surf., B* **2013**, *110*, 138; c) Q. Tang, Y. Yao Xu, J. Dong Wu, J. Sun, J. Wang, J. Jun Xu, J. Feng Deng, *J. Controlled Release* **2006**, *114*, 41; d) E. Juere, G. Del Favero, F. Masse, D. Marko, A. Popat, J. Florek, R. Caillard, F. Kleitz, *Eur. J. Pharm. Biopharm.* **2020**, *151*, 171; e) K. K. Bansal, D. K. Mishra, A. Rosling, J. M. Rosenholm, *Appl. Sci.* **2020**, *10*, 289.

[28] a) H. Laroui, S. A. Ingersoll, H. C. Liu, M. T. Baker, S. Ayyadurai, M. A. Charania, F. Laroui, Y. Yan, S. V. Sitaraman, D. Merlin, *PLoS One* **2012**, *7*, e32084; b) B. Chassaing, J. D. Aitken, M. Malleshappa, M. Vijay-Kumar, *Curr. Protoc. Immunol.* **2014**, *104*, 25.

[29] a) I. Slowing, B. G. Trewyn, V. S. Lin, *J. Am. Chem. Soc.* **2006**, *128*, 14792; b) W. Zeng, X. F. Qian, Y. B. Zhang, J. Yin, Z. K. Zhu, *Mater. Res. Bull.* **2005**, *40*, 766.

[30] a) J. Yang, L. Zhou, L. Zhao, H. Zhang, J. Yin, G. Wei, K. Qian, Y. Wang, C. Yu, *J. Mater. Chem.* **2011**, *21*, 2489; b) C. M. Yang, P. H. Liu, Y. F. Ho, C. Y. Chiu, K. J. Chao, *Chem. Mater.* **2003**, *15*, 275.

[31] a) R. Lofberg, P. Rutgeerts, H. Malchow, C. Lamers, A. Danielsson, G. Olaison, D. Jewell, O. Ostergaard Thomsen, H. Lorenz-Meyer, H. Goebell, H. Hodgson, T. Persson, C. Seidegard, *Gut* **1996**, *39*, 82; b) M. Campieri, A. Ferguson, W. Doe, T. Persson, L. G. Nilsson, *Gut* **1997**, *41*, 209.

[32] I. Okayasu, S. Hatakeyama, M. Yamada, T. Ohkusa, Y. Inagaki, R. Nakaya, *Gastroenterology* **1990**, *98*, 694.

[33] a) J. Fallingborg, L. A. Christensen, B. A. Jacobsen, S. N. Rasmussen, *Dig. Dis. Sci* **1993**, *38*, 1989; b) A. G. Press, I. A. Hauptmann, L. Hauptmann, B. Fuchs, M. Fuchs, K. Ewe, G. Ramadori, *Aliment. Pharmacol. Ther.* **1998**, *12*, 673.

[34] a) H. Ali, B. Weigmann, M. F. Neurath, E. M. Collnot, M. Windbergs, C. M. Lehr, *J. Controlled Release* **2014**, *183*, 167; b) H. Zhou, H. Qian, *Drug Des. Dev. Ther.* **2018**, *12*, 2601.

[35] a) G. Barbara, Z. Xing, C. M. Hogaboam, J. Gauldie, S. M. Collins, *Gut* **2000**, *46*, 344; b) R. Kuhn, J. Lohler, D. Rennick, K. Rajewsky, W. Muller, *Cell* **1993**, *75*, 263; c) R. de Waal Malefyt, J. Abrams, B. Bennett, C. G. Figdor, J. E. de Vries, *J. Exp. Med.* **1991**, *174*, 1209; d) S. Schreiber, T. Heinig, H. G. Thiele, A. Raedler, *Gastroenterology* **1995**, *108*, 1434; e) S. Melgar, M. M. Yeung, A. Bas, G. Forsberg, O. Suhr, A. Oberg, S. Hammarstrom, A. Danielsson, M. L. Hammarstrom, *Clin. Exp. Immunol.* **2003**, *134*, 127; f) B. Li, R. Alli, P. Vogel, T. Geiger, *J. Immunol.* **2013**, 190; g) Y. Gu, J. Yang, X. Ouyang, W. Liu, H. Li, J. Yang, J. Bromberg, S. H. Chen, L. Mayer, J. C. Unkeless, H. Xiong, *Eur. J. Immunol.* **2008**, *38*, 1807; h) M. Djaldetti, H. Bessler, *Int. J. Immunol. Immunother.* **2018**, *5*, 6.

[36] B. Li, R. Alli, P. Vogel, T. L. Geiger, *Mucosal Immunol.* **2014**, *7*, 869.

[37] S. Yang, L. Zhao, C. Yu, X. Zhou, J. Tang, P. Yuan, D. Chen, D. Zhao, *J. Am. Chem. Soc.* **2006**, *128*, 10460.

[38] J. Lu, M. Liong, J. I. Zink, F. Tamanoi, *Small* **2007**, *3*, 1341.

[39] J. Kecht, A. Schlossbauer, T. Bein, *Chem. Mater.* **2008**, *20*, 7207.

[40] a) C. T. Nguyen, R. I. Webb, L. K. Lambert, E. Strounina, E. C. Lee, M. O. Parat, M. A. McGuckin, A. Popat, P. J. Cabot, B. P. Ross, *ACS Appl. Mater. Interfaces* **2017**, *9*, 9470; b) Y. Krishnamachari, P. Madan, S. Lin, *Int. J. Pharm.* **2007**, *338*, 238.

[41] a) M. Perse, A. Cerar, *J. Biomed. Biotechnol.* **2012**, *2012*, 718617; b) B. Chassaing, J. D. Aitken, M. Malleshappa, M. Vijay-Kumar, *Curr. Protoc. Immunol.* **2014**, *104*, 15251.

[42] a) R. Eri, M. A. McGuckin, R. Wadley, *Methods Mol. Biol.* **2012**, *844*, 261; b) N. Pujara, K. Y. Wong, Z. Qu, R. Wang, M. D. Moniruzzaman, P. Rewatkar, T. Kumeria, B. P. Ross, M. McGuckin, A. Popat, *Mol. Pharmaceutics* **2020**, DOI: 10.1021/acs.molpharmaceut.0c00048.